Scaling of Suction Feeding Performance in the Catfish *Clarias gariepinus*[*]

Sam Van Wassenbergh[†]
Peter Aerts
Anthony Herrel
Department of Biology, University of Antwerp, Universiteitsplein 1, B-2610 Antwerp, Belgium

Accepted 8/11/2005; Electronically Published 11/11/2005

ABSTRACT

Ontogenetic changes in the absolute dimensions of the cranial system together with changes in kinematics during prey capture can cause differences in the spatiotemporal patterns of water flow generated during suction feeding. Because the velocity of this water flow determines the force that pulls prey toward and into the mouth cavity, this can affect suction feeding performance. In this study, size-related changes in the suction-induced flow patterns are determined. To do so, a mathematical suction model is applied to video recordings of prey capturing *Clarias gariepinus* ranging in total length from 111 to 923 mm. Although large *C. gariepinus* could be expected to have increasing peak velocities of water flow compared with small individuals, the results from the hydrodynamic model show that this is not the case. Yet, when *C. gariepinus* becomes larger, the expansive phase is prolonged, resulting in a longer sustained flow. This flow also reaches farther in front of the mouth almost proportionally with head size. Forward dynamical simulations with spherical prey that are subjected to the calculated water flows indicate that the absolute distance from which a given prey can be sucked into the mouth as well as the maximal prey diameter increase substantially with increasing head size. Consequently, the range of potential prey that can be captured through suction feeding will become broader during growth of *C. gariepinus*. This appears to be reflected in the natural diet of this species, where both the size and the number of evasive prey increase with increasing predator size.

[*] This article was presented at the symposium "The Ontogeny of Performance in Vertebrates," Seventh International Congress of Vertebrate Morphology, Boca Raton, Florida, 2004.

[†] Corresponding author; e-mail: sam.vanwassenbergh@ua.ac.be.

Physiological and Biochemical Zoology 79(1):43–56. 2006. 1522-2152/2006/7901-4096$15.00

Introduction

Suction feeding is the most commonly used prey capture mechanism in aquatic vertebrates (e.g., Lauder 1985; Ferry-Graham and Lauder 2001). To generate suction, animals rapidly expand their bucco-pharyngeal cavity, resulting in a flow of water into the mouth (Muller et al. 1982; Muller and Osse 1984; Aerts et al. 2001; Ferry-Graham et al. 2003). During successful strikes, this water flow exerts enough drag force onto the prey to accelerate it toward the mouth, where it is caught between the oral jaws or completely engulfed and transported through the mouth cavity. Because drag forces increase with the velocity of the water flow, generating a sufficiently high suction flow speed is a critical aspect of prey capture success in suction feeders (Svanbäck et al. 2002).

Because the dimensions of the bucco-pharyngeal cavity change through ontogeny, the hydrodynamics of suction feeding will most likely change as well. Obviously, animals with a larger head will be able to displace a larger amount of water by expanding their larger feeding apparatus. However, scaling effects on the speed of the suction-induced flow are less obvious. If we consider an isometrically growing animal fully expanding its bucco-pharyngeal apparatus in a constant period of time, the following relationships apply: (1) the rate of bucco-pharyngeal volume change will increase proportionally with the cube of the body length, while (2) the surface area of the mouth aperture, through which the water has to flow, increases only with the square of the body length. Consequently, if we assume that the flow velocity is proportional to the ratio of rate of volume change to the area of the opening through which it flows (Muller et al. 1982; Van Leeuwen and Muller 1984), suction flow speed at the mouth aperture would increase linearly with body size. Thus, large animals seem to have a considerable advantage over small animals when it comes to generating high suction flow speeds.

On the other hand, like most other movements of the musculoskeletal system, cranial expansions are subject to scaling effects on the velocity of movement as well. Large animals will inevitably become slower in performing a movement that is similar relative to its body size (Hill 1950; Schmidt-Nielson 1984). In addition, muscle physiology experiments have demonstrated the slowing down of the maximal intrinsic muscle contraction velocity during growth within a single species (James et al. 1998) and also across a broad sample of species with increasing adult body size (Medler 2002). Consequently, it is not surprising that during feeding in teleost fishes (Richard

and Wainwright 1995; Wainwright and Shaw 1999; Hernandez 2000) and sharks (Robinson and Motta 2002), the time it takes to complete a given expansion of the jaws or hyoid apparatus increases as animals become larger (but see Reilly 1995).

Because of the opposing effects of the increase in expansion volume relative to mouth aperture (increasing flow speed) and the relative slowing down of movement during growth (decreasing flow speed), it is hard to predict how suction feeding performance will change during ontogeny. Although there are several studies on how prey capture kinematics of aquatic vertebrates change through ontogeny (Richard and Wainwright 1995; Cook 1996; Hunt Von Herbing et al. 1996; Wainwright and Shaw 1999; Hernandez 2000; Robinson and Motta 2002), none of these have addressed how the observed changes in feeding kinematics may result in changes in the suction-induced flow. However, the characteristics of this flow are critical determinants of the capture success during a suction event.

Thus, the aim of this article is to compare the velocity of the suction flow during prey capture in a broad size range of African catfish (*Clarias gariepinus*) and use this to evaluate scaling effects on suction performance. Because there is considerable information available on the natural diet of *C. gariepinus* (Bruton 1979), we can further examine whether changes in suction performance are reflected in changes in the diet during growth in this species.

Material and Methods

Study Animals

Clarias gariepinus is an air-breathing catfish (Family Clariidae) with an almost Pan-African distribution that can also be found in rivers and lakes of the Middle East and Turkey (Teugels 1996). It has a broad diet that includes mostly fishes, shrimps, crabs, insect nymphs, beetles, and snails (Bruton 1979). While this species shows different kinds of foraging behaviors, such as individual bottom feeding, surface feeding, or group hunting, prey are generally captured by a combination of suction feeding and biting (Bruton 1979; Van Wassenbergh et al. 2004). Juvenile *C. gariepinus* specimens already have a fully ossified cranial system that appears to be generally similar in shape to the adult configuration at the ontogenetic stage of 127 mm standard length (Adriaens and Verraes 1998). Adults can grow up to 1.5 m total length (Teugels 1986), making this species particularly suitable for studying scaling effects.

In this study, we used 17 individuals of between 110.8 and 923.0 mm in total length. Because the cranial length (defined as the distance between the rostal tip of the premaxilla and the caudal tip of the occipital process) can be measured more precisely and excludes variability in the length of body and tail, we will further use this metric to quantify size. The individuals used were either aquarium-raised specimens obtained from the

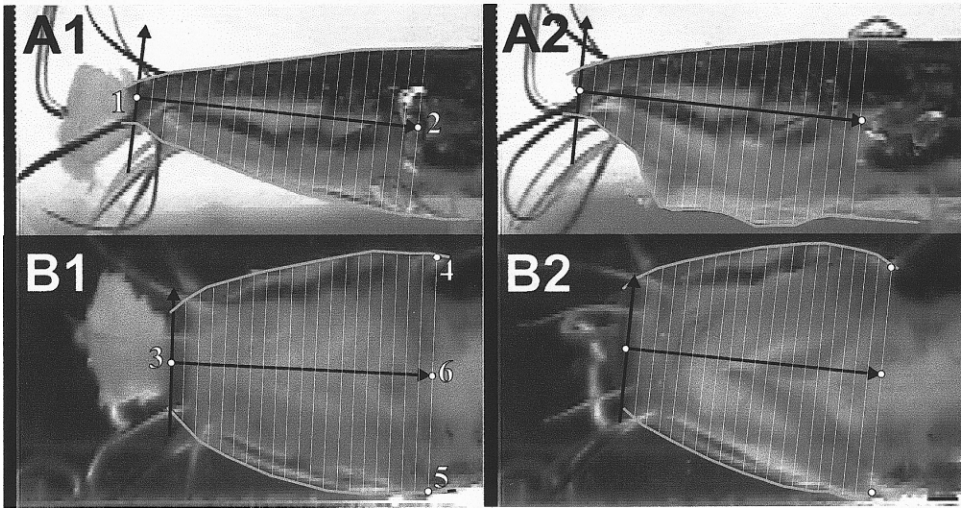

Figure 1. Selected frames from a prey capture sequence of *Clarias gariepinus* recorded simultaneously in lateral (*A1*, *A2*) and ventral view (*B1*, *B2*), illustrating the measurements that were made and used as input variables in the suction model (*A1*, *B1*: before the start of suction; *A2*, *B2*: after prey intake). The gray lines represent the curves that fitted through the digitized coordinates of the contours of the head. The black arrows represent the fish-bound frame of reference of which the longitudinal axis runs from landmarks (*white points with numbers*) *1* to *2* in lateral view (see *A1*) and from landmarks *3* to *6* in ventral view (see *B2*). The positions of the landmarks digitized are (*1*) the upper jaw tip at the side of the mouth opening, (*2*) the anterior tip of the base of the pectoral fin, (*3*) the middle of the mouth aperture, (*4*) and (*5*) the anterior tips of the bases of the right and left pectoral fins, and (*6*) the middle between landmarks *4* and *5*. The distance along the longitudinal axis from mouth aperture to pectoral fin base was divided into 21 equally spaced intervals for which the height (*white lines in A1 and A2*) and the width (*white lines in B1 and B2*) of the head were calculated. These values constituted the minor and major axis of the ellipse base area of an elliptical cylinder. In our model, the volume changes over time of these 21 serially arranged elliptical cylinders were assumed to correspond to volume changes of the mouth cavity.

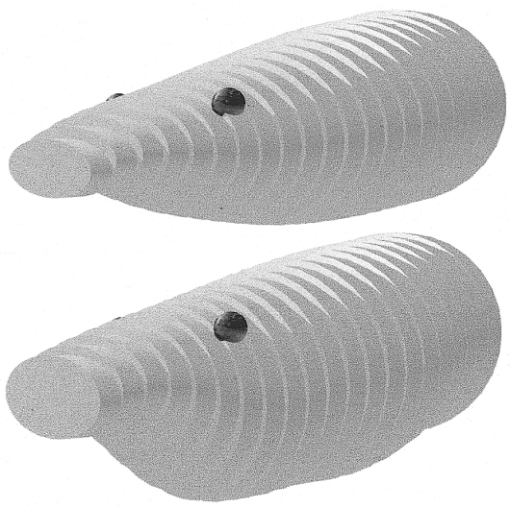

Figure 2. Three-dimensional illustration of the head-volume of *Clarias gariepinus* as modeled by a series of elliptical cylinders. The compressed (*top*) and expanded (*bottom*) volumes correspond to the images shown in Figure 1.

Laboratory for Ecology and Aquaculture (Catholic University of Leuven) or specimens obtained from aquacultural facilities (Fleuren and Nooijen BV, Someren, The Netherlands). All animals were kept in a separate aquarium during the course of the training and recording period. In general, it took about 2 wk to train the catfish to feed regularly in a restricted part of the aquarium.

Video Recordings of Prey Captures

Video sequences were recorded of *C. gariepinus* capturing pieces of cod (*Gadus morhua*) that were pinned onto a plastic coated steel wire. In order to obtain a similar feeding situation for both the small and large individuals, the size of the prey was scaled according to the size of the catfish (diameter between 25% and 35% of cranial length). The recordings were made using a Redlake Imaging Motionscope digital high-speed video camera at 250 frames per second (for individuals with cranial lengths between 28.01 and 71.00 mm), a JVC GR-DVL9800 camera at 100 frames per second (for the individuals with cranial lengths of 94.13 and 130.0 mm), or a Panasonic F15 at 50 frames per second (for the 210.2 mm cranial length individual). The feeding sequences were recorded simultaneously in lateral and ventral view using a mirror placed at 45°. Two floodlights (600 W) provided the necessary illumination. Only those prey capture sequences that were approximately perpendicular to the camera lens were selected and retained for further analysis.

Ten recordings were analyzed for each individual. From these video sequences, the velocity of hyoid depression was determined. This was done by measuring the distance between the eye and the tip of the hyoid for each consecutive frame (using Didge, version 2.2.0; A. Cullum). For species with a dorsoventrally flattened head such as *C. gariepinus*, the depression of the hyoid apparatus is likely the most important expansive event of suction (Alexander 1970; Lauder 1985). Consequently, the sequences in which an individual shows the highest velocity of hyoid depression most likely correspond to the sequences in which suction effort is maximized. Therefore, for each individual, only the two sequences with the highest and second highest peak velocity of hyoid depression were further analyzed using the suction model detailed below.

Suction Model

To calculate the water velocities inside the mouth cavity and in front of the fishes' mouths, we used the ellipse model of Drost and van den Boogaart (1986). Using this method, estimation of the flow volume can be considerably improved over previous model estimations (Drost and van den Boogaart 1986). It has shown to give accurate predictions of flow velocities in suction feeding larval carp (*Cyprinus carpio*; Drost and van den Boogaart 1986) and in the snake-necked turtle (*Chelodina longicollis*; Aerts et al. 2001). Also for suction feeding of *C. gariepinus*, we have indications that this model gives good predictions of the actual flow velocity. Preliminary results of a high-speed x-ray video analysis of *C. gariepinus* capturing small, spherical pieces of shrimp (6 mm diameter) charged with a small steel marker (0.5 mm diameter) show maximal prey velocities of 1.2 m/s. After applying the suction model (see below for details) to the same individual, the two analyzed sequences gave maximal flow velocities of 1.13 and 1.60 m/s. Assuming that small prey behave approximately as a part of the fluid, these findings suggest that also for *C. gariepinus*, the model output is (at least) realistic.

In our suction model, the head of the catfish, from mouth aperture to pectoral fin, is approximated by a series of 21 elliptical cylinders. Each elliptical cylinder has an ellipse-shaped base area from which the length of the major and minor axis, respectively, correspond to the height and width of the head at any given position (Figs. 1, 2). Changes in the length of both axes were deduced from the recorded videos. To do so, upper and lower contours of the catfishes' head were digitized frame by frame (50 points each) in the lateral and ventral view. At the same time, the coordinates of a longitudinal axis connecting the upper jaw tip to the middle between left and right pectoral fin bases were digitized (for more information, see Fig. 1). Next, the contour coordinates were recalculated in a new frame of reference moving along with the fish, with the upper jaw tip as the origin and the longitudinal axis as the *X*-axis. The coordinates of each curve were then fitted with tenth-order polynomial functions using the XlXtrFun add-in for Microsoft Excel (Advanced System Design and Development, Red Lion, PA). With these functions, at 21 equally spaced intervals along the

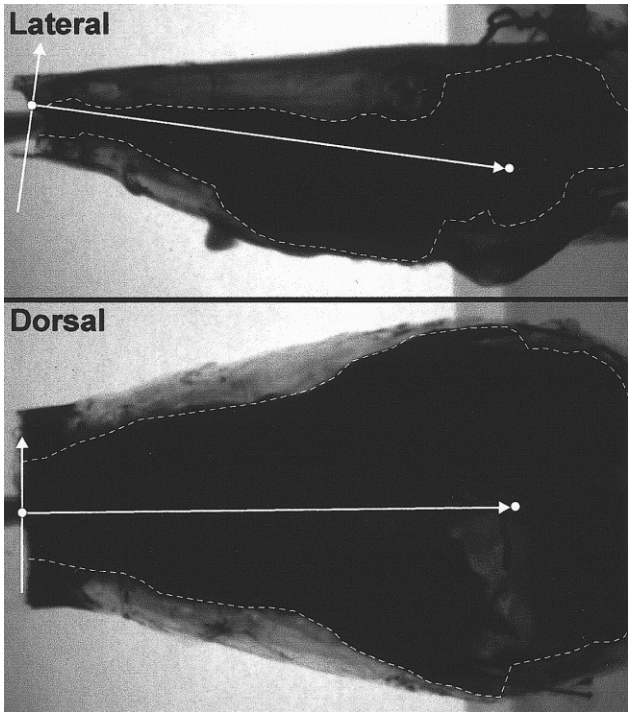

Figure 3. Lateral and dorsal x-ray photographs used to measure the internal dimensions of the unexpanded mouth cavity of a preserved *Clarias gariepinus* specimen (cranial length = 94.13 mm). The internal contours of the mouth cavity (*dashed lines*) were quantified by filling the mouth with a radio-opaque barium solution. The same frame of reference (*white arrows representing the axes*) as in the external video analysis (see Fig. 1) was used to determine the height and the width of the mouth cavity at the specific positions along the longitudinal axis defined in Figure 1.

longitudinal axis (starting with mouth aperture until pectoral fins), the distance between the corresponding coordinates of the upper and lower contours were calculated (Fig. 1). With these data, changes in the width and height of the ellipses over time as well as changes in the volume of the elliptical cylinders were calculated. For each elliptical cylinder, the profiles of length and width versus time were filtered with a fourth-order Butterworth zero phase shift low-pass filter in order to reduce digitization noise (cut-off frequency of 30, 12, and 6 Hz for videos recorded at 250, 100, and 50 Hz). Figure 2 gives an idea of how the volume of the catfishes' head is represented in the model.

The internal dimensions of the mouth cavity of *C. gariepinus* in rest are approximated using x-ray images from lateral and ventral view x-ray videos of a preserved specimen (Fig. 3). During recording of these x-ray videos, the specimen was held vertically while a saturated barium solution was poured in the mouth. Using this radio-opaque fluid, the boundaries of the mouth cavity could accurately be distinguished, and the internal area of the mouth cavity could be determined for all positions along the longitudinal axis at the base of each elliptical cylinder (Fig. 1). Again, internal areas were approximated by ellipses consisting of the height and width of the measured distance between the upper and lower contours of the internal volume on the lateral and ventral x-ray images at these positions (Fig. 3). To account for the presence of the gill apparatus, the length of the major and minor axes of ellipses in the gill region were (arbitrarily) reduced by 10%. It was assumed that this situation (i.e., the internal volume of the mouth cavity of the preserved specimen at rest) reflects the moment before start of the suction event. Subsequently, changes in the height and the width of the head over time (calculated as in Fig. 1) will cause changes in the width and height of the internal mouth volume ellipses. Because internal volume data were collected only for one individual, we are forced to assume that the dimensions of the bucco-pharyngeal cavity are proportional to the measured external dimensions of the head in *C. gariepinus*. The x-ray videos were made with a Philips Optimus x-ray generator coupled to a Redlake Imaging Motionpro digital high-speed camera.

If we assume that the volume of the tissues in the head remains constant, changes in the volume of the head correspond to equal changes in the volume of the mouth cavity. According to the continuity principle, any change in volume must be filled instantaneously with water and thus generate a flow relative to the fishes' head. Thus, at each cross section of the mouth cavity, the total water volume passing through this cross section in a given amount of time depends on the total volume increase posterior to this cross section. In this way, the average flow velocity during a given time increment can be calculated at each of the modeled ellipse-shaped cross sections of the mouth cavity by dividing the volume increase posterior to this ellipse by the area of the ellipse (average for that time increment). This holds as long as the opercular and branchiostegal valves are closed. If not, the modeled system becomes undetermined (Muller et al. 1982; Muller and Osse 1984; Drost and van den Boogaart 1986). In general, valve opening can be detected shortly after *C. gariepinus* reaches maximal oral gape. However, for several of the recorded prey capture sequences, it was problematic to pinpoint exactly the frames in which the transition from closed to opened valves occurred. Therefore, we used the model output only from the start of mouth opening until the time of maximal gape.

To calculate flow velocity in front of the mouth, the following formula from Muller et al. (1982) is used:

$$v = \frac{(v_m h^3)}{(d^2 + h^2)^{1.5}},$$

with v the flow velocity in the direction of the longitudinal axis, v_m the flow velocity at the mouth aperture (both v and v_m in the earth-bound frame), h the radius of the mouth opening (assumed to be circular), and d the distance from the mouth at which the velocity is calculated. In this way, the flow around

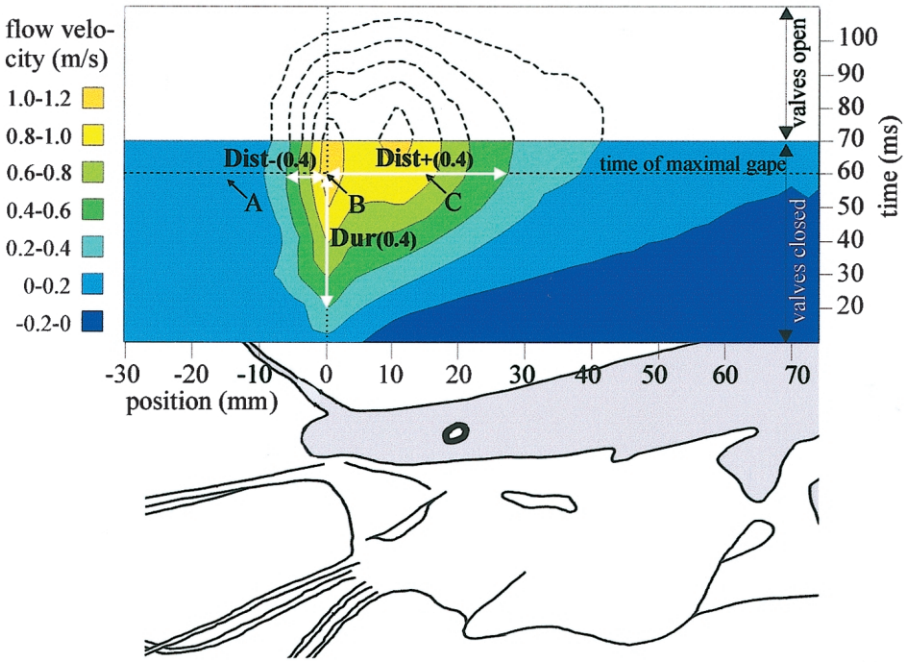

Figure 4. Spatiotemporal flow velocity patterns (in fish-bound frame of reference) outside and inside the buccal cavity (position is illustrated by the drawing below the graph), as predicted by the model for a prey capture sequence of a 94.1 mm cranial length *Clarias gariepinus*. Note that the model is unreliable after valve opening, and therefore only the flow pattern before the time of the maximum gape was used. Variables quantifying peak suction flow speed, suction distance, and suction duration are indicated by arrows in the center of the graph. *Dist− (0.4)* and *Dist+ (0.4)* represent maximal distance outside and inside the mouth that is subject to a flow velocity of 0.4 m/s or more. *Dur(0.4)* gives the duration in which a flow velocity of 0.4 m/s is sustained before the time of maximum gape at the level of the mouth aperture. *A* and *C* are peak flow velocity at a position of 0.168 × cranial length outside and inside of the mouth aperture. *B* indicates the peak flow velocity at the mouth aperture.

the mouth opening is modeled as a circular vortex filament (see Muller et al. 1982). Given the relatively slow forward movement of *C. gariepinus* during prey capture (average peak forward velocity of 0.096 m/s), the complexity of the model and the data interpretation could be reduced by assuming that the observed cranial expansions occur in stationary catfish. The diameter of the mouth opening is calculated as the mean of the height and width of the mouth. The height of the mouth was measured by digitizing the interior sides of the upper and lower jaw on the lateral view images. Because this external flow velocity decreases approximately proportionally with the cube of the distance away from the mouth, flow velocity will rapidly drop in front of the expanding mouth cavity. Recent experiments using the particle image velocimetry technique have demonstrated that this indeed is the case for suction feeding fishes (Ferry-Graham et al. 2003).

Quantification and Comparison of Flow Characteristics

Because the model gives a spatiotemporal pattern of water flow velocities (Fig. 4), specific quantifications of the characteristics of this pattern are needed in order to compare the model output for the different-sized catfish. These quantifications are illustrated in Figure 4, together with an example of the model output. Four types of variables were defined: (1) peak suction flow speeds: the maximal flow speeds at specific positions (fixed positions expressed in millimeters as well as relative distances expressed in numbers of cranial lengths) along the longitudinal axis (−15 mm, 0 mm, +15 mm, −0.168 cranial lengths, and +0.168 cranial lengths; negative positions are in front of the mouth, positive positions are inside of the mouth); (2) external suction distance: the maximal distance in front of the mouth at which specific flow speeds (0.2, 0.4, 0.6, and 0.8 m/s) take place; (3) internal suction distance: the maximal distance inside of the mouth cavity (measured from the mouth aperture) in which specific flow speeds (0.2, 0.4, 0.6, and 0.8 m/s) can still occur; and (4) suction duration: the amount of time during which specific flow speed levels (0.2, 0.4, 0.6, and 0.8 m/s) can be sustained at the mouth aperture. An illustration of how these variables are determined from the model output is shown in Figure 4. Because we are interested only in maximal suction performance, the highest value for each of these variables from the two modeled prey capture sequences per individual was used for in the subsequent regression analyses.

Table 1: Scaling relationships of 17 variables quantifying the spatiotemporal flow pattern from suction modeling of *Clarias gariepinus*

Variable	Slope	R^2	P	95% Confidence Limits	
				Lower	Upper
Peak flow velocity:					
15 mm outside	2.47	.79	<.0001	1.78	3.18
.168 CL outside	−.32	.16	.1089	−.73	.08
Mouth aperture	−.33	.21	.0614	−.69	.02
15 mm inside	.94	.65	<.0001	.56	1.31
.168 CL inside	−.24	.13	.1627	−.60	.11
Maximum outside distance:					
.2 m/s flow	.86	.89	<.0001	.69	1.03
.4 m/s flow	.84	.84	<.0001	.64	1.04
.6 m/s flow	.79	.72	<.0001	.52	1.06
.8 m/s flow	.69	.44	.0037	.26	1.12
Maximum inside distance:					
.2 m/s flow	.86	.90	<.0001	.70	1.02
.4 m/s flow	.85	.82	<.0001	.63	1.07
.6 m/s flow	.85	.76	<.0001	.59	1.10
.8 m/s flow	.81	.45	.0033	.32	1.31
Duration:					
.2 m/s flow	.89	.88	<.0001	.71	1.07
.4 m/s flow	.80	.73	<.0001	.53	1.07
.6 m/s flow	.58	.19	.0841	−.09	1.26
.8 m/s flow	.25	.3	.4875	−.49	.98

Note. P denotes the probability of the slope differing from 0. Outside and inside refer to the positions in front of the fish and internal of the buccal cavity, respectively. All distances are with regard to the mouth aperture (see Fig. 4). $N = 17$. CL = cranial length.

Additionally, the forward velocity (in earth-bound frame of reference) of the catfish during prey capture was analyzed. Although this is not directly an aspect of the inertial suction process (displacing water relative to the fish by expanding the bucco-pharyngeal volume), any size-dependent changes in the attack strategy can influence scaling effects on prey capture performance. For example, a study by Cook (1996) showed that a juvenile cottid fish (*Clinocottus analis*) shifts from a ram-dominant feeding mode (relying more on fast swimming toward the prey) to a suction-dominant feeding mode during ontogeny. In this case, by focusing on only the flow patterns relative to the fish, an important behavioral component of prey capture performance could be overlooked. Therefore, the average peak horizontal velocity in the direction of the prey as well as maximum peak horizontal velocity (out of all 10 sequences per individual) were analyzed for scaling effects. These velocities were determined from the digitized coordinates of the middle of the eye after noise filtering (Butterworth low-pas filtering) and differentiation versus time.

Because growth is an exponential phenomenon, all data were $\log_{10}$-transformed values (one data point for each individual) and plotted against the $\log_{10}$ of cranial length. Next, least squares regressions were performed on these data. Because the model output (dependent data) likely has a much greater error than measurements of cranial length (independent data), least squares regressions are appropriate in this case (Sokal and Rohlf 1995). The slopes of these linear regressions with 95% confidence limits were determined in order to evaluate changes in aspects of the flow regime in relation to changes in body size. A slope of 0 means that the variable is independent of cranial length. Slopes of 1 and −1 denote that the variables increase or decrease proportional to cranial length, while a slope of 2 stands for a variable increasing with the square of cranial length. The significance level of $P = 0.05$ was used throughout the analysis. Because the existing statistical methods that account for multiple testing (e.g., sequential Bonferroni correction) are incorrect in ignoring the number of significant tests in the analysis (Moran 2003), we did not reduce the significance level in case of high percentages of significant results at $P = 0.05$ (see, e.g., Table 1).

Simulations of Prey Displacement

A number of forward dynamical simulations were performed for a hypothetical prey that is subjected to the calculated spatiotemporal flow velocity patterns. In these simulations, drag forces resulting from the suction-induced water flow move the prey. The following equation of motion is used:

$$(m_{\text{prey}} + m_{\text{added}}) \times a_{\text{prey}} = \frac{1}{2} C_{\text{d}} A \rho v_{\text{r}}^2 + \frac{3}{2} \rho V_{\text{prey}} a_{\text{fluid}},$$

where m_{prey} is the mass of the prey, m_{added} an added mass component, a_{prey} the acceleration of the prey, C_{d} the shape-dependent drag coefficient, A the frontal area of the prey (area projected onto a plane perpendicular to the direction of fluid flow), ρ the density of the fluid (1,000 kg/m^3), v_{r} the linear velocity of the water flow relative to the prey, V_{prey} the volume of the prey, and a_{fluid} the acceleration of the fluid at the position of the prey.

Because the hydrodynamic properties of natural prey are immensely diverse, it is impossible to account for this diversity. For example, the difference in frontal area A and C_{d} for a fish parallel or the same fish perpendicular to the flow is considerable. Therefore, if standardized, spherical prey with the same density as the fluid are used in the simulations, gravitational force and hydrostatical lift will cancel each other out, and the problem will essentially reduce to the displacement of a fluid particle. This prey is presented at a specific position in front of the fish's mouth at the longitudinal axis used in the suction

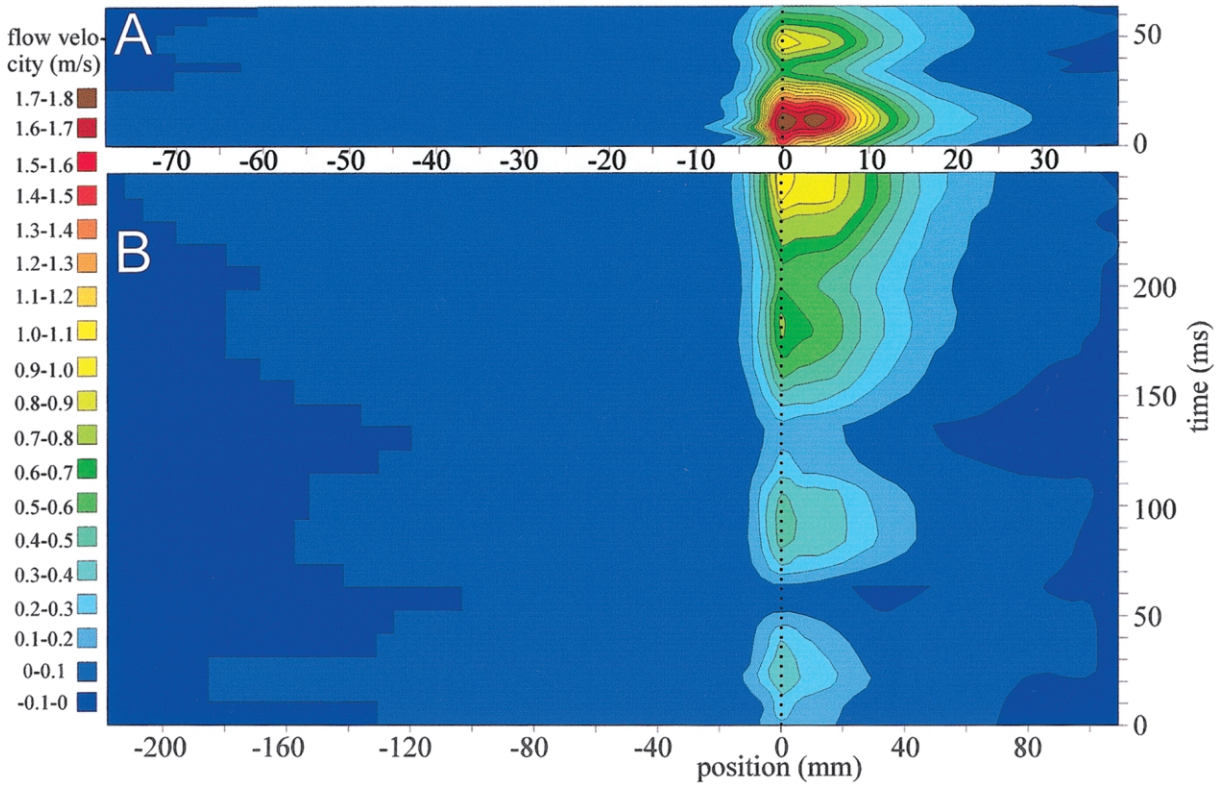

Figure 5. Examples of representative spatiotemporal flow velocity patterns from individuals of 46 mm (*A*) and 130 mm (*B*) cranial length. The dotted line (at 0 mm position) corresponds to the mouth aperture (see also Fig. 4). Note that the horizontal axis (position) is scaled according to the cranial lengths of the two individuals.

model and is immobilized until the time corresponding to one frame after the start of the cranial expansion (first time for which flow velocity can be calculated). Because the suction model output gives flow velocities only at discrete positions along the longitudinal axis (intervals of 0.042 cranial lengths) rather than a continuous function, linear interpolations were used to calculate flow velocity at any given position. The simulations were stopped at one frame after the time of maximal gape (end of suction flow calculations). The added mass of a spherical particle with the same density of the surrounding water equals half the mass of this particle (Daniel 1984). The drag coefficient of a sphere depends on its Reynolds number ($\mathrm{Re} = D\rho v_r/\eta$, with D the diameter of the sphere, ρ the density of the water, v_r the flow velocity relative to the sphere, and η the dynamic viscosity of water (0.001 kg/m/s; Vogel 1994) and is approximated by the following formula from White (1991):

$$C_d = \frac{24}{\mathrm{Re}} + \frac{6}{1 + \mathrm{Re}^{0.5}} + 0.4,$$

with $0 < \mathrm{Re} < 2 \times 10^5$. Because the results will show that the horizontal velocity of *C. gariepinus* toward the prey does not change significantly with size (see further), this was not taken into account in the modeled predator-prey interaction.

We assumed that the modeled flow velocity at the position of the center of the sphere is uniform over the entire sphere and that the flow itself is not influenced by the presence of the prey. These assumptions will hold only for small prey relative to the size of the mouth opening. Thus, it should be kept in mind that these simulations merely predict how a standardized prey would behave in a given modeled flow pattern rather than giving realistic predictions of prey displacement in the course of a suction feeding sequence. The goal of these simulations is to evaluate how the differences in flow pattern characteristics could potentially be translated to differences in prey movement. Because the objective of this study is to compare fishes of different sizes, these simplifications seem justified.

Results

The flow velocity patterns predicted by the suction model clearly change with increasing fish size. The most conspicuous changes can easily be illustrated by comparing the model output for small and large fish (Fig. 5). When *Clarias gariepinus* becomes larger, the duration of the expansive phase becomes

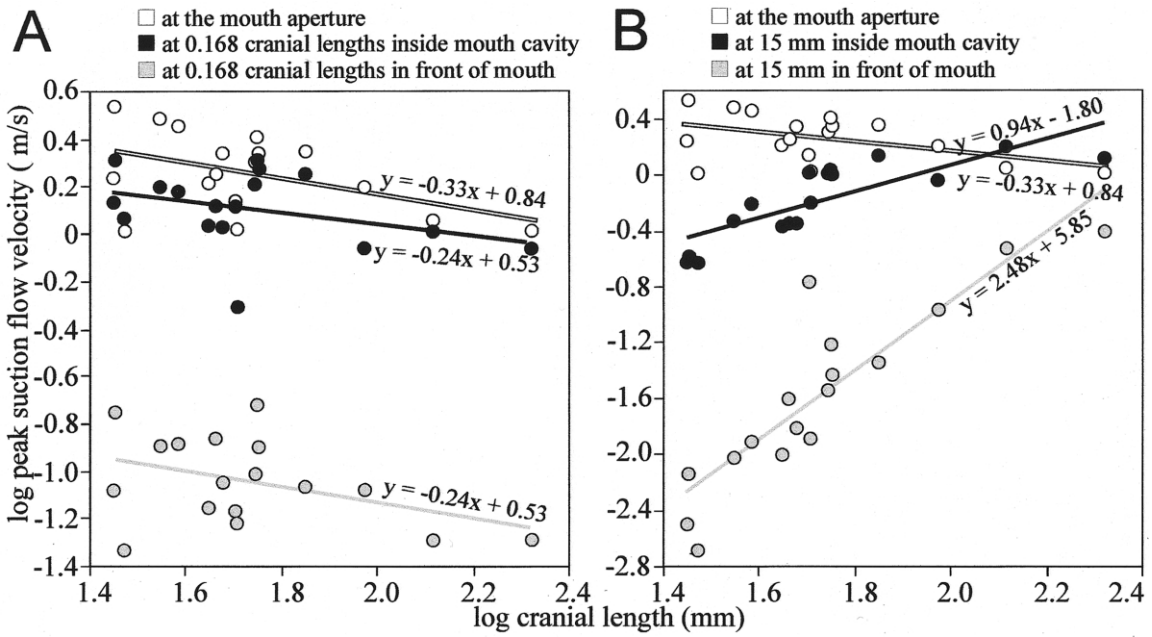

Figure 6. Log-log plots of peak suction flow velocities against cranial length, as predicted by the suction model for the positions as represented in the legend above each graph. Least squares regression lines with equations are shown for each variable. While *A* represents scaling relationships at distances relative to the size of the catfishes' cranium, *B* gives scaling relationships of maximal flow velocities at fixed, absolute distances away from the mouth aperture. See Table 1 for a summary of these data.

longer, resulting in a prolonged time during which suction can be generated (Fig. 5). Second, in larger individuals, flow reaches farther away from the mouth aperture both outside and within the mouth cavity (Fig. 5).

Maximal Suction Velocities

Although the slope of the least squares regression suggests a decrease in the peak flow velocities at the mouth aperture (Fig. 6), this relation is statistically not significant ($P = 0.061$). Also, for the peak flow velocities at fixed absolute distances from the mouth aperture proportional to cranial size (Fig. 6*A*), no significant changes with changing cranial size can be demonstrated (Table 1).

In contrast, a different result is found when comparing peak suction flow speeds at distances from the mouth aperture (Fig. 6*B*). For flow 15 mm inside the mouth, peak flow speed scales with a slope of 0.94, which is an almost proportional increase with cranial length. An even more rapid increase of maximal flow velocity with head size is found in front of the mouth opening (Fig. 6*B*). Fifteen millimeters in front of the mouth, peak flow speed increases with cranial length to the exponent 2.47.

Suction Distance

Suction distance in front of the mouth (Fig. 7*A*) and inside of the mouth cavity (Fig. 7*B*) show very similar scaling relationships. A close correspondence is also found between scaling of the different flow velocities (Fig. 7; Table 1). In general, scaling exponents vary around 0.8, which means an increase of suction distance roughly proportional with size. However, because all 95% confidence limits include the slope of 1 (Table 1), suction distance does not decrease significantly relative to the fishes' head size.

Suction Duration

Before maximum gape, the low suction-induced flow speeds (0.2 and 0.4 m/s) are sustained for a longer time in larger *C. gariepinus* individuals (Fig. 8). This increase is almost proportional to body length (regression slopes of 0.88 and 0.80, respectively). For the higher flow velocities (0.6 and 0.8 m/s), the sustainable duration seems to scale differently (slopes of 0.58 and 0.25, respectively; Fig. 8). However, a much larger inter-individual variability in the model output occurs for these two variables. Because the error of the slopes is considerable, both a scaling-independent relationship (slope 0) and a scaling proportional to body size (slope 1) cannot be excluded for the duration of the two highest flow velocities that were compared in this study (Table 1).

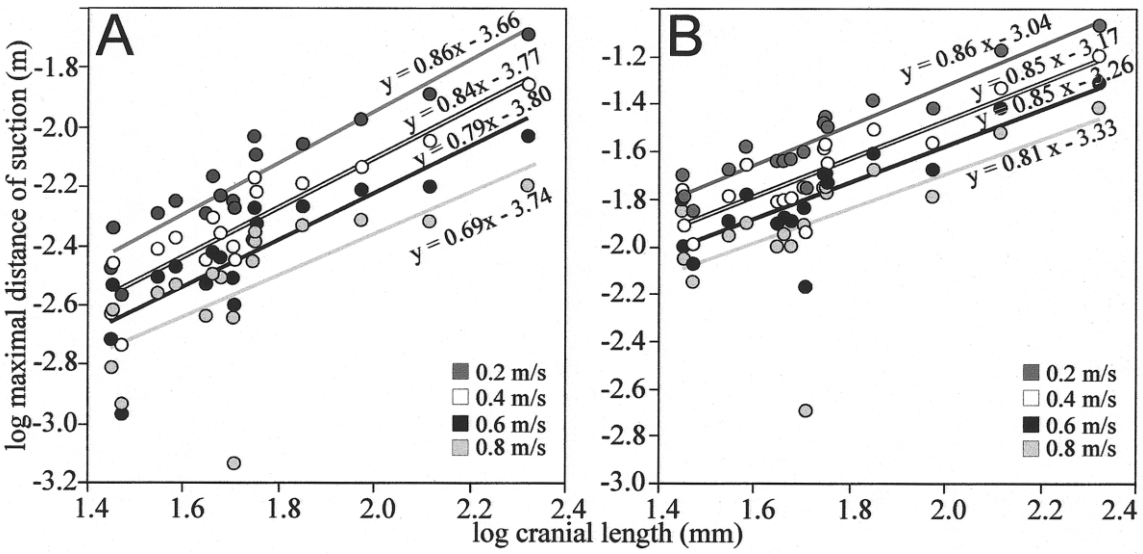

Figure 7. Log-log plots of maximal external (*A*) and internal (*B*) suction distance against cranial length, as predicted by the model for four levels of flow velocity (legends in the lower right-hand corner of each graph). Least squares regression lines with equations are shown for each variable. All distances are measured from the mouth aperture (see also Fig. 4). See Table 1 for a summary.

Attack Velocity

No significant change in the peak horizontal velocity in the direction of the prey during prey capture was found with changing cranial size (Fig. 9). For the average peak velocity and the maximal peak velocity (out of 10 strikes per individual), slopes of the linear regressions were 0.16, with 95% confidence limits between −0.16 and 0.46 for both variables ($N = 17$; $R^2 = 0.08$). However, when expressed as relative velocities (in cranial lengths per second), small fishes are considerably faster compared with large fishes (slope = −0.84, $N = 17$; $R^2 = 0.71$; 95% confidence interval between −1.14 and −0.54).

Discussion

Scaling of Spatiotemporal Flow Characteristics

The model predicts that maximal flow speed during suction of *Clarias gariepinus* does not increase with increasing size of the cranial system. Moreover, the results of the model even show a decreasing trend with increasing size (Fig. 6*A*; Table 1). Two factors can contribute to this result. First, when *C. gariepinus* becomes larger, a relatively smaller expansion of the mouth cavity might occur during the expansive phase. For example, if a catfish of double length expands only to a four times larger volume (half of its capacity expected from isometry) in the same amount of time, then the model will predict equal flow speeds. Second, when *C. gariepinus* grows, scaling effects on prey capture kinematics may cause the slowing down of the cranial expansions, as shown in other fish taxa (Richard and Wainwright 1995; Cook 1996; Hunt Von Herbing et al. 1996; Wainwright and Shaw 1999; Hernandez 2000). For example, if it takes twice as long for the double-size catfish to generate a given volume expansion, flow velocities will also stay equal.

For *C. gariepinus*, a combination of these two factors appears to apply. First, smaller individuals generate a relatively larger expansion of their mouth cavity. If we plot the total volume change (model output at the time of maximum gape minus volume at the start of prey capture) against cranial length in a $\log_{10}$-$\log_{10}$ graph, we did not find the expected isometric slope of 3 but 2.31 (95% confidence limits: 1.70 and 2.91). Second, the duration of the expansive phase (defined here as time until maximum gape) increases considerably with rising cranial size (slope of 0.86 for the 34 analyzed sequences, 95% confidence limits: 0.62 and 1.09). Separately, neither of these two factors is enough to explain the observed result for peak flow velocity (Fig. 6*A*). However, the combination of a less extensive cranial expansion and a longer time to create this expansion for the larger *C. gariepinus* causes the peak flow speed to remain constant when compared with the smaller individuals of this species.

In contrast, at fixed absolute distances away from the mouth aperture, large *C. gariepinus* individuals do have a substantial advantage over small ones when it comes to generating higher suction flow velocities (Fig. 6*B*). It should be noted that for such variables, the observed scaling relationships depend on how fast the flow velocity drops at a certain distance away from the mouth aperture. Figure 10 illustrates this situation for a theoretical flow velocity pattern in front of the mouth, which is determined by the formula from Muller et al. (1982; see "Material and Methods"). For this flow pattern, scaling relationships depend on the distance from the mouth aperture but

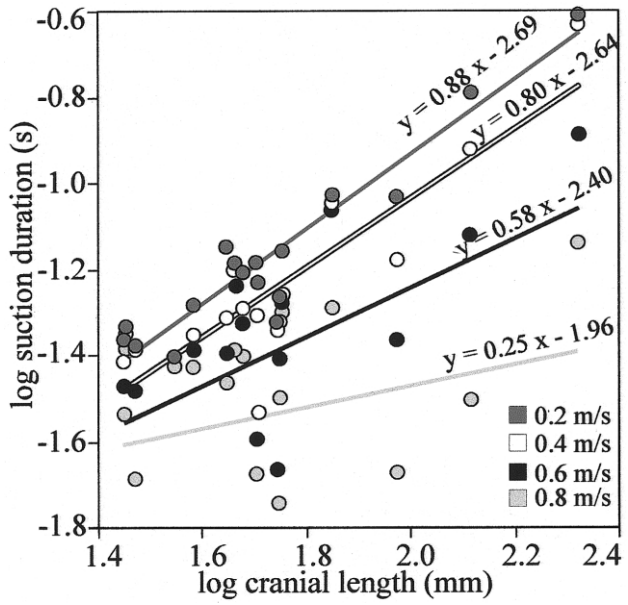

Figure 8. Log-log plot of suction duration against cranial length, as predicted by the model for four levels of flow velocity (legend in the lower right-hand corner of the graph). Least squares regression lines with equations are shown for each variable. Suction duration is measured at the mouth aperture (see Fig. 4). See Table 1 for a summary.

also on the size range of animals used in the study (Fig. 10). For example, if we had selected a distance farther away from the mouth, less steep scaling regressions would be found. Also, for the peak suction velocities at relative distances in front of the mouth aperture, the observed scaling effects depend on the fraction of cranial length that is chosen but are independent of the used size range of fish (Fig. 10). This is just to show that almost any extrapolation of the observed scaling effects for variables of peak flow speeds distant from the mouth aperture will likely be incorrect. Although not representative of the scaling relationships of the entire flow pattern, each of these variables does have a clear biological relevance in determining the magnitude of the drag forces that pull the prey toward and into the mouth at a given point along the longitudinal axis of the expansive system.

Suction distance in *C. gariepinus* scales slightly less than proportional to cranial size (Fig. 7). For the external suction distance (in front of the mouth opening), this scaling relationship is a result of the circular vortex filament model (Muller et al. 1982) included in our model calculations. Inherent to this model, the maximal distances to which low suction flow velocities reach show a relatively faster increase with increasing absolute mouth opening size (Fig. 10) when compared with high flow velocities. Consequently, this trend is also observed in the scaling data of *C. gariepinus* (Fig. 7; Table 1). For the internal suction distance (inside the mouth cavity), with similar peak flow velocities at the mouth aperture, we would expect an increase proportional to cranial length. Although the results are not statistically different from these expectations (Table 1), the scaling exponents tend to be somewhat lower. Most likely, this is related to the decreasing trend in the peak values of flow velocity at the mouth aperture (Fig. 6).

The fact that suction duration increases during growth (Fig. 8) is obviously related to the prolonged time between the start of the cranial expansion and the time at which this expansion is completed. As mentioned earlier, the time between the onset and offset (time of maximum gape) of the model increases almost proportionally with cranial length. As a result, specific flow velocities can be kept up for a considerably longer time when *C. gariepinus* becomes larger (Figs. 5, 8).

Scaling of Suction Performance

Although it is obvious that data describing patterns of water flow during prey capture are critical for understanding the impact of movements of the head on the water surrounding the prey (Ferry-Graham and Lauder 2001), induced water velocities are merely proximate measures of suction feeding performance (Wainwright et al. 2001). Indeed, the calculated variables quantifying the changes in the spatiotemporal flow velocity pattern with changing head size (Figs. 6–8) do not directly predict the outcome of the interaction between the moving water, prey, and predator. However, if flow velocity in function of time and position is known, movement of a hypothetical prey subjected to this flow can be reconstructed. Indeed, forward dynamic simulations of prey displacement allow us to explore the importance of the size-related changes in flow velocity for prey displacement.

The maximal distance to which flow reaches away from the mouth aperture was found to scale slightly less than proportional to cranial size (Fig. 7*A*). However, this does not directly mean that prey can be caught from farther away, because such prey have to be moved over a larger distance and for a longer period of time. In other words, a very short, far-reaching burst of flow velocity may not be sufficient to achieve prey transport from its outermost points. To evaluate this, a spherical prey of 4 mm diameter was introduced into the calculated flow patterns. Next, the maximal distance away from the mouth opening for which this prey could still reach the mouth aperture during the course of the expansive phase was calculated. The results of these simulations are given in Figure 11*A*. Consistent with the scaling relationships of maximum flow distance in front of the mouth aperture (Fig. 7), the calculated maximum distance from which the 4-mm sphere can reach the mouth opening at the time of maximal gape scales with an exponent of 0.86 ($N = 17$; $R^2 = 0.87$; 95% confidence intervals between 0.68 and 1.04). This indicates that the ability to capture prey from farther away from the mouth by suction feeding in *C. gariepinus* increases with cranial size. The simulations even predict that this distance of suction increases nearly proportional

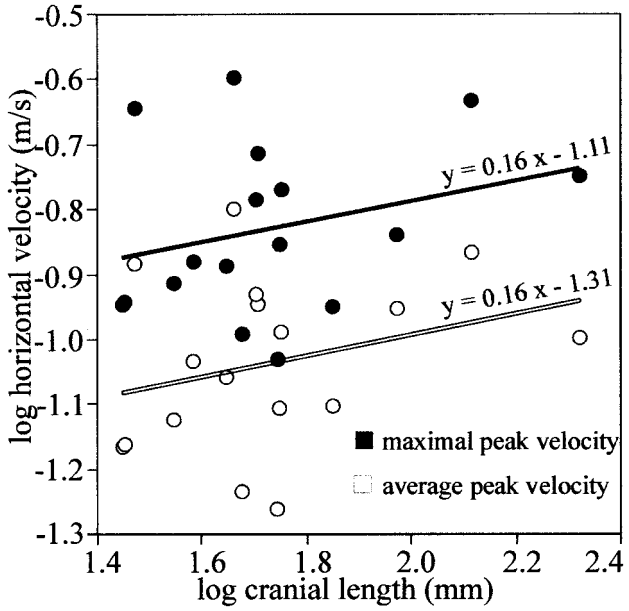

Figure 9. Log-log plot of the peak horizontal velocity of *Clarias gariepinus* during prey approach against cranial length. Data are shown for the maximum and average values (legend in the lower right-hand corner of the graph).

with cranial length (Fig. 11*A*). This is not entirely surprising if we consider that behavioral observations have shown that this species often initiates prey capture upon contact with the barbels (Bruton 1979; Van Wassenbergh et al. 2004) and that the length of these chemo-sensitive structures projecting from the mouth increases along with size of the cranium.

Large fish have a larger absolute gape compared with small individuals of the same species. This allows these large individuals to feed on larger prey compared with small ones (Schael et al. 1991; Huskey and Turingan 2001; Magnhagen and Heibo 2001). However, when prey size increases, its moment of inertia will increase as well. Consequently, higher suction-induced drag forces on the prey will be necessary to accelerate larger prey to a given velocity. To evaluate for *C. gariepinus* how the maximal size of prey is limited by the scaling effects on the suction flow pattern, spherical prey were presented into the calculated flow patterns at a distance of 5 mm in front of the mouth aperture. Next, the maximal diameter of the prey for which this prey could still reach the position of 10 mm inside of the mouth cavity (measured from the mouth aperture) during the course of the expansive phase was calculated. The results of these simulations are given in Figure 11*B*. The maximal size of the sphere that can still perform this movement scales to cranial length with an exponent of 1.63 ($N = 14$; $R^2 = 0.41$; 95% confidence intervals between 0.41 and 2.86). These simulations suggest that during growth of *C. gariepinus*, its ability to capture larger prey by suction feeding increases substantially. According to the model's predictions, maximal prey size would even increase faster than proportional to cranial size if these prey are sucked from the same absolute distance from the mouth (Fig. 11*B*).

So far, it seems that the flow patterns generated by *C. gariepinus* increase the efficiency to capture prey by suction feeding during ontogeny from juveniles to large adults (Fig. 11). Moreover, our results indicate that whenever a fish swims at a certain distance in front of the mouth of a *C. gariepinus* individual, it will have a reduced chance of escaping when it concerns a large catfish compared with a small catfish. This increased suction performance appears also to be reflected in the dietary data from the literature on *C. gariepinus*. Bruton (1979) compared stomach contents from different size classes of *C. gariepinus* from a South African lake and found increasing proportions (dry weight) of fish and decreasing proportions of insects and mollusks in the diet with increasing predator size. Moreover, individuals larger than 700 mm total length included only fish in their diet (Bruton 1979). Because the success of capturing fast and evasive prey (such as fish) depends more on maximal suction feeding performance compared with other prey, the

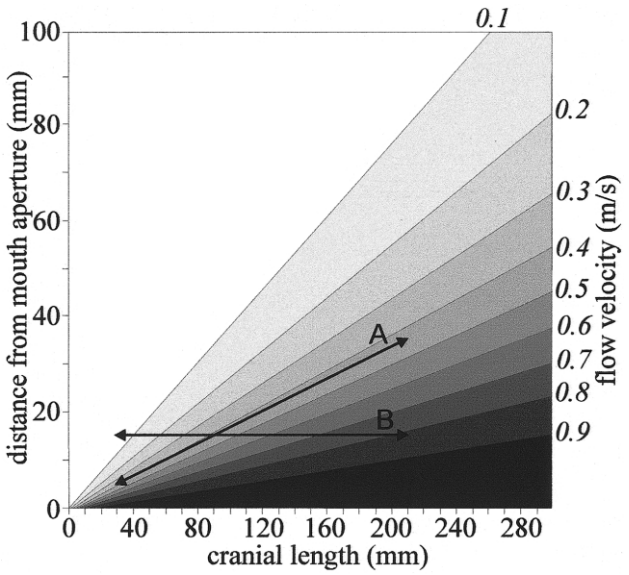

Figure 10. Theoretical illustration of the decreasing flow velocity exterior of the mouth opening in relation to cranial size, resulting from the circular vortex filament model of Muller et al. (1982) for a flow velocity at the mouth aperture of 1 m/s and a mouth opening radius of 0.2 times cranial length. Arrow *A* represents the data range included in the peak flow velocity scaling relationships at relative distance of 0.168 cranial lengths away from the mouth opening (given in Fig. 6*A*). Arrow *B* corresponds to the data range from the scaling relations of peak flow speed at fixed absolute distance of 15 mm. Arrows that are parallel to *A* or *B* but at another position on the graph can easily cross a different number of isovelocity lines. This indicates that scaling effects depend on the chosen distance and, only for *B*, also on the size range of animals used in the analysis.

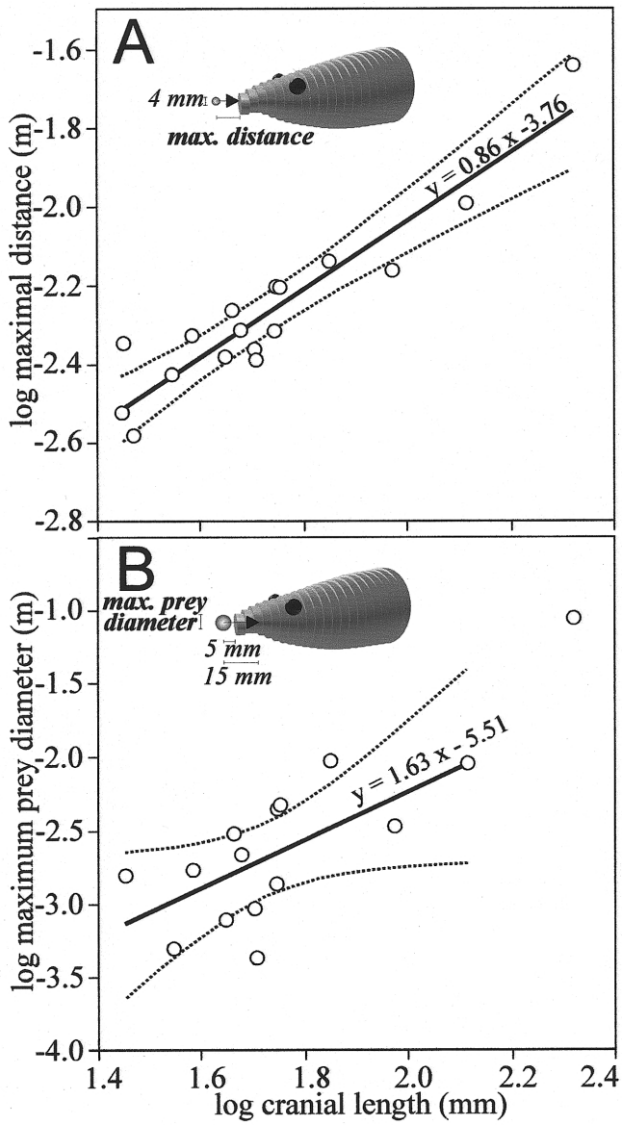

Figure 11. Log-log plots of maximal prey distance (*A*) and maximal prey size (*B*) versus cranial length, as predicted by forward dynamic simulations of spherical prey moving in the deduced flow fields. In *A*, the hypothetical prey has a fixed diameter length of 4 mm. In *B*, the starting distance was set at 5 mm in front of the mouth. Least squares regression lines with equations and 95% confidence limits (*dotted lines*) are shown. Note that in *B*, the value for the largest individual was not included in the regression, since a sphere of 90 mm close to the mouth will interfere with the cranial expansions.

observed shift in the diet may be a direct consequence of the scaling relationships presented here. Furthermore, while the presented scaling results indicate an increase (with increasing head size) in the maximum size of prey that can be drawn into the mouth cavity by suction (Fig. 11*B*), the diet study of Bruton (1979) also found the size of the most common prey (*Sarotherodon mossambicus*) increasing linearly with predator length. Thus, changes in suction feeding capacity seem to be reflected in the properties of the natural diet of *C. gariepinus*.

At this point, we have focused only on absolute differences in suction feeding performance, that is, when small and large fish feed on prey of the same absolute size or at the same absolute distance from the mouth. However, small fish will probably aim at smaller prey and will also be able to approach prey closer compared with large fish. Hence, suction performance was also compared for a situation that is similar relative to the predators' size, that is, with prey size and initial distance from the mouth in proportion to cranial length. In that case, the simulations show that the small fishes clearly outperform the larger fishes (Fig. 12).

There are several reasons for this negative scaling relationship (Fig. 12). First, prey inertia increases with the cube of the prey's length, while drag forces increase only with the square of prey length. This means that when prey size increases in proportion with predator size, higher drag forces (and thus higher suction flow velocities) are needed for the larger predators to generate similar prey accelerations compared with smaller predators. If we exclude this factor from the simulations by artificially scaling mass and added mass to the cube of cranial length, there is still a significant decrease in realized relative prey displacement

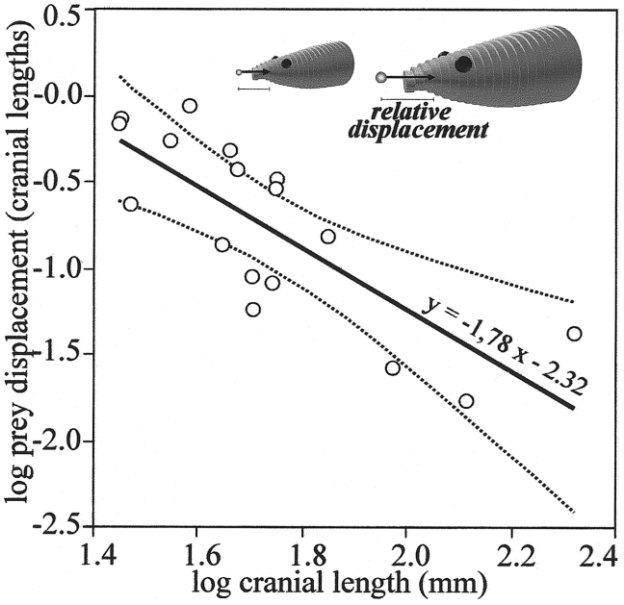

Figure 12. Log-log plot of total relative prey displacement (in numbers of cranial lengths) against cranial length, as predicted by forward dynamic simulations of spherical prey moving in the calculated flows. In order to create a situation with similar conditions relative to the size of each individual, initial prey distance in front of the mouth and prey diameter were adjusted in proportion to cranial length (10% and 5%, respectively, of cranial length). Least squares regression lines with equations and 95% confidence limits (*dotted lines*) are shown (R^2 = 0.62; 95% confidence intervals between −1.01 and −2.54).

with increasing cranial size (slope = −0.782, $N = 17$; $R^2 = 0.41$; 95% confidence intervals between −0.01 and −1.55), though less strong (Fig. 12). This remaining negative scaling relationship must be caused by scaling effects on the suction-induced flow velocity. Indeed, our results have shown that peak values of suction flow velocity tend to decrease (Fig. 6*A*) and that also the distance to which a given flow velocity can reach away from the mouth aperture does not scale proportionally to head length (Fig. 7). Both of these results can contribute to the decreasing performance when prey capture situations are isometrically upscaled with head size.

Because relative forward velocity of the predator also decreases with size (Fig. 9), these simulations potentially even underestimate the scaling effects on prey capture performance in this situation. On the other hand, if the spherical prey is representing a prey fish before its escape response, a decrease in speed, acceleration, and maneuverability during the subsequent escape of this prey with increasing prey size can be expected (Domenici 2001), which may cancel out the relatively faster approach from the predator. Not only evasiveness and size of prey but also behavioral aspects of both predator (e.g., foraging mode) and prey (e.g., predator perception capacity) will be important, because these determine potential scaling effects on the distance from which the predator is forced to initiate its prey capture. This illustrates that the study of scaling relationships of prey capture performance is extremely complex, because several aspects of the predator-prey interaction can have an influence on the outcome of a suction feeding event.

As long as we have no idea of how suction distance, prey size, and predator size are interrelated, the ecological relevance of mathematical simulation with isometrically scaled prey size and distance can be questioned. Yet, our simulations do demonstrate that small *C. gariepinus* are not at all the poor suction feeders as may appear from Figure 11. If they specialize on prey with a size in proportion to their own size, and if the initial distance can be reduced accordingly, their prey capture success will still be very high. Still, the results from the simulations with varying absolute distances and prey sizes (Fig. 11) illustrate their limitations when it comes to feeding on prey that are larger or farther away. In this way, scaling effects on suction-induced flow velocities will restrict smaller individuals to a smaller subset of the potential prey spectrum in the environment when compared with the larger individuals.

Acknowledgments

We thank D. Adriaens for comments on the manuscript. W. Fleuren is acknowledged for supplying *Clarias gariepinus* specimens. Thanks to F. Ollevier, F. Volckaert, and E. Holsters for providing us with *C. gariepinus* larvae and also the largest individual used in this study. We gratefully acknowledge support of the Special Research Fund of the University of Antwerp. A.H. is a postdoctoral fellow of the Fund for Scientific Research, Flanders (FWO-Vl).

Literature Cited

Adriaens D. and W. Verraes. 1998. Ontogeny of the osteocranium in the African catfish, *Clarias gariepinus* Burchell (1822) (Siluriformes, Clariidae): ossification sequence as a response to functional demands. J Morphol 235:183–237.

Aerts P., J. Van Damme, and A. Herrel. 2001. Intrinsic mechanics and control of fast cranio-cervical movements in aquatic feeding turtles. Am Zool 41:1299–1310.

Alexander R.McN. 1970. Mechanics of the feeding action of various teleost fishes. J Zool (Lond) 162:145–156.

Bruton M.N. 1979. The food and feeding behaviour of *Clarias gariepinus* (Pisces: Clariidae) in Lake Sibaya, South Africa, with emphasis on its role as a predator of cichlid fishes. Trans Zool Soc Lond 35:47–114.

Cook A. 1996. Ontogeny of feeding morphology and kinematics in juvenile fishes: a case study of the cottid fish *Clinocottus analis*. J Exp Biol 199:1961–1971.

Daniel T.L. 1984. Unsteady aspects of aquatic locomotion. Am Zool 24:121–134.

Domenici P. 2001. The scaling of locomotor performance in predator-prey encounters: from fish to killer whales. Comp Biochem Physiol A 131:169–182.

Drost M.R. and J.G.M. van den Boogaart. 1986. A simple method for measuring the changing volume of small biological objects, illustrated by studies of suction feeding by fish larvae and of shrinkage due to histological fixation. J Zool (Lond) 209:239–249.

Ferry-Graham L.A. and G.V. Lauder. 2001. Aquatic prey capture in ray-finned fishes: a century of progress and new directions. J Morphol 248:99–119.

Ferry-Graham L.A., P.C. Wainwright, and G.V. Lauder. 2003. Quantification of flow during suction feeding in bluegill sunfish. Zoology 106:159–168.

Hernandez L.P. 2000. Intraspecific scaling of feeding mechanics in an ontogenetic series of zebrafish, *Danio rerio*. J Exp Biol 203:3033–3043.

Hill A.V. 1950. The dimensions of animals and their muscular dynamics. Sci Prog 38:209–230.

Hunt Von Herbing I., T. Miyake, B.K. Hall, and R.G. Boutilier. 1996. Ontogeny of feeding and respiration in larval Atlantic cod *Gadus morhua* (Teleostei: Gadiformes). II. Function. J Morphol 227:37–50.

Huskey S.H. and R.G. Turingan. 2001. Variation in prey-resource utilization and oral jaw gape between two populations of largemouth bass, *Micropterus salmoides*. Environ Biol Fishes 61:185–194.

James R.S., N.J. Cole, M.L.F. Davies, and I.A. Johnston. 1998. Scaling of intrinsic contractile properties and myofibrillar

protein composition of fast muscle in the fish *Myoxocephalus scorpius* L. J Exp Biol 201:901–912.

Lauder G.V. 1985. Aquatic feeding in lower vertebrates. Pp. 210–229 in M. Hildebrand, D.M. Bramble, K.F. Liem, and D.B. Wake, eds. Functional Vertebrate Morphology. Belknap, Cambridge, MA.

Magnhagen C. and E. Heibo. 2001. Gape size allometry in pike reflects variation between lakes in prey availability and relative body depth. Funct Ecol 15:754–762.

Medler S. 2002. Comparative trends in shortening velocity and force production in skeletal muscles. Am J Physiol Regul Integr Comp Physiol 283:368–378.

Moran M.D. 2003. Arguments for rejecting the sequential Bonferroni in ecological studies. Oikos 100:403–405.

Muller M. and J.W.M. Osse. 1984. Hydrodynamics of suction feeding in fish. Trans Zool Soc Lond 37:51–135.

Muller M., J.W.M. Osse, and J.H.G. Verhagen. 1982. A quantitative hydrodynamic model of suction feeding in fish. J Theor Biol 95:49–79.

Reilly S.M. 1995. The ontogeny of aquatic feeding behavior in *Salamandra salamandra*: stereotypy and isometry in feeding kinematics. J Exp Biol 198:701–708.

Richard B.A. and P.C. Wainwright. 1995. Scaling the feeding mechanism of largemouth bass (*Micropterus salmoides*): kinematics of prey capture. J Exp Biol 198:419–433.

Robinson M.P. and P.J. Motta. 2002. Patterns of growth and the effects of scale on the feeding kinematics of the nurse shark (*Gynglymostoma cirratum*). J Zool (Lond) 256:449–462.

Schael D.M, L.G. Rudstam, and J.R. Post. 1991. Gape limitation and prey selection in larval yellow perch (*Perca flavescens*), freshwater drum (*Aplodinotus grunniens*), and black crappie (*Promoxis nigromaculatus*). Can J Fish Aquat Sci 48:1919–1925.

Schmidt-Nielson K. 1984. Scaling: Why Is Animal Size So Important? Cambridge University Press, Cambridge.

Sokal R.F. and F.J. Rohlf. 1995. Biometry. W.H. Freeman, New York.

Svanbäck R., P.C. Wainwright, and L.A. Ferry-Graham. 2002. Linking cranial kinematics, buccal pressure, and suction feeding performance in largemouth bass. Physiol Biochem Zool 75:532–543.

Teugels G.G. 1986. Clariidae. Pp. 66–101 in J. Daget, J.P. Gosse, and D.F.E.T. Van Den Audenaerde, eds. Checklist of the Freshwater Fishes of Africa (Cloffa). Vol. 2. Institut Royal des Sciences Naturelles de Belgique, Brussels; Musée Royal de l'Afrique Centrale, Tervuren; and Office de la Recherche Scientifique et Technique Outre-Mer, Paris.

———. 1996. Taxonomy, phylogeny and biogeography of catfishes (Ostariophysi, Siluroidei): an overview. Aquat Living Resour 9:9–34.

Van Leeuwen J.L. and M. Muller. 1984. Optimum sucking techniques for predatory fish. Trans Zool Soc Lond 37:137–169.

Van Wassenbergh S., A. Herrel, D. Adriaens, and P. Aerts. 2004. Effects of jaw adductor hypertrophy on buccal expansions during feeding of air breathing catfishes (Teleostei, Clariidae). Zoomorphology 123:81–93.

Vogel S. 1994. Life in Moving Fluids: The Physical Biology of Flow. Princeton University Press, Princeton, NJ.

Wainwright P.C., L.A. Ferry-Graham, T.B. Waltzek, A.M. Carroll, D.C. Hulsey, and J.R. Grubich. 2001. Evaluating the use of ram and suction during prey capture by cichlid fishes. J Exp Biol 204:3039–3051.

Wainwright P.C. and S.S. Shaw. 1999. Morphological basis of kinematic diversity in feeding sunfishes. J Exp Biol 202:3101–3110.

White F.M. 1991. Viscous Fluid Flow. 2nd ed. McGraw-Hill, New York.